

## GEOLOGICAL LINEAMENT INTERPRETATION USING THE OBJECT-BASED IMAGE ANALYSIS APPROACH: RESULTS OF SEMI-AUTOMATED ANALYSES VERSUS VISUAL INTERPRETATION

by  
*Maarit Middleton<sup>1)</sup>, Tilo Schnur<sup>2)</sup>, Peter Sorjonen-Ward<sup>3)</sup> and Eija  
Hyvönen<sup>1)</sup>*

**Middleton, M., Schnur, T., Sorjonen-Ward, P. & Hyvönen, E. 2015.** Geological lineament interpretation using the object-based image analysis approach: Results of semi-automated analyses versus visual interpretation. *Geological Survey of Finland, Special Paper 57*, 135–154, 8 figures.

Structural interpretation is an essential part of a mineral exploration project because the genesis of many mineralization types is controlled by bedrock structures. The objective of this study was to detect weakness and deformation zones of bedrock on a regional scale from remotely sensed magnetic and digital elevation datasets. Firstly, Object-Based Image Analysis (OBIA) is introduced in the detection of local elongated minima from aeromagnetic data, the most commonly used data in regional structural interpretation in Finland. Secondly, visual lineament interpretation results of the magnetic data and high-resolution digital elevation model acquired by laser scanning are presented from the Enontekiö study area in NW Finland. Finally, the lineament detection processes are reviewed against the literature. An OBIA algorithm called the Object-Based Lineament Detection (OBLD) implemented in eCognition software was developed with Cognitive Network Language (CNL) to delineate continuous tilt derivative (TDR) minima for pattern recognition of the weakness zones from aeromagnetic data. The success of the method relies on line extraction raster filtering. However, the algorithm is not quite as sensitive in finding local minima of TDR as curvature analysis (Phillips et al. 2007) for detecting edges from potential field data. The results of this paper also imply that visual interpretation cannot currently be excluded or replaced by semi-automated image processing techniques in the lineament detection of gridded geophysical or topographic data. Visual interpretation and pattern recognition-based lineament detection methods should be considered complementary rather than exclusive, although pattern recognition methods provide a more objective first-pass interpretation of lineaments compared to visual techniques. Further work in lineament detection in mineral exploration should focus on applying both new and established pattern recognition methods, gearing towards the use of a variety of geophysical and remotely sensed data sources, and the representation of these results as an integrated lineament interpretation approach for evaluation and interpretation by structural geologists.

Keywords (GeoRef Thesaurus, AGI): lineaments, structural analysis, magnetic properties, laser scanning, image analysis, Enontekiö, Finland

- <sup>1)</sup> Geological Survey of Finland, P.O. Box 77, FI-96101 Rovaniemi, Finland,  
e-mail: [maarit.middleton@gtk.fi](mailto:maarit.middleton@gtk.fi), tel. +358 (0)29 503 4345;  
e-mail: [eija.hyvonen@gtk.fi](mailto:eija.hyvonen@gtk.fi), +358 (0)29 503 4226
- <sup>2)</sup> Trimble Geospatial, Trimble Geospatial Division, Arnulfstrasse 126,  
80636 Munich, Germany,  
e-mail: [Tilo\\_Schnur@Trimble.com](mailto:Tilo_Schnur@Trimble.com), +49 89 8905 71426
- <sup>3)</sup> Geological Survey of Finland, P.O. Box 1237, FI-70211 Kuopio, Finland,  
e-mail: [peter.sorjonen-ward@gtk.fi](mailto:peter.sorjonen-ward@gtk.fi), +358 (0)29 503 3750

## INTRODUCTION

The recognition of geological linear structures such as bedrock fault and shear zones, thrust faults, fractures, lithological contacts and fold structures is essential when exploring for mineral deposits, or more subtle indications of mineralizations. The majority of mineral deposits are controlled or affected by geological structures, and epigenetic mineralization styles in particular tend to be structurally controlled or constrained. The relative importance of different types of structures varies between mineral deposits. However, major crustal faults are necessary in the transportation of the large volume of fluids required for the genesis of a significant ore body. Zones of weakness, i.e. shear zones and reverse faults or thrusts, are important in mineral exploration because of their potential to transport and focus mineralized fluids. The spatial proximity to zones of structural weakness and intersections between major structures and zones of weakness, or boundaries between lithological units are also of potential interest in exploration (e.g., Pagel & Leroy 1991, Bierlein et al. 2006). Therefore structural mapping, and especially the detection of weakness and fracture zones, is a vital part of an exploration project. In Finland, weakness zones divide the Precambrian shield into bedrock blocks of different scales. Some of these are associated with neotectonic movements due to crustal rebound during and after the last deglaciation, but they may also represent the reactivation of older weakness zones (see e.g., Ojala et al. 2004, Mäkelä 2012) and therefore have significance in mineral exploration.

The linear and curve-linear appearance of tectonic structures visible in remotely sensed data sources has captured the attention of geoscientists for decades. This brand of geosciences is called lineament detection, as originally introduced by Hobbs (1904, in O'Leary et al. 1976). It is considered as the recognition of lineaments, i.e. "mappable, simple or composite linear features of a surface, whose parts are aligned in a rectilinear or slightly curvilinear relationship and which differs distinctly from the patterns of adjacent features and presumably reflects a subsurface phenomenon" (O'Leary et al. 1976). In areas of thick overburden and limited bedrock exposure, such as the formerly glaciated terrain of Fennoscandia, lineament detection over regional extents is only possible by interpretation of remotely sensed

geophysical and topographic data and needs to be undertaken prior to field campaigns and drilling. In better-exposed areas, the interpretation of such data may more readily be complemented by field observations than in regions with sediment cover.

Geological structures can be recognized from a variety of remotely sensed datasets. Magnetic, gravity, radiometric, visible and near infrared, imaging radar and topographic data sources are frequently used. Globally, the detection of topographic lineaments is most commonly used, due to a lack of relevant geophysical data. Topographic lineaments can be observed as elongated depressions with varying widths or elongated abrupt steps in surface elevation (see e.g., Mäkelä 2012). They may be observed from a variety of data sources, including digital elevation models (DEM, e.g., Abarca 2006), very high resolution optical data from unmanned aerial vehicles (Stumpf et al. 2013), high (Sukumar et al. 2014) or medium resolution from satellites (Koike et al. 1998, Kocal et al. 2007), synthetic aperture radar data (SAR, Gloaguen et al. 2007), and SAR interferometry (Hooper et al. 2003). In optical data, the spectral response of topographic lineaments comes from shadowing, though non-topographic lineaments may also be discernible through vegetation, which changes according to the moisture conditions. In tectonically active areas, lineaments can be observed to have a thermal infrared response (Ouzounov et al. 2006, Papadaki et al. 2011). However, in Finland, problems in systematic mapping are encountered in areas of thick sediment cover and in the precise positioning of lineaments in wide valleys (see e.g., Mäkelä 2012). Lineaments having a physical response can be detected with a variety of geophysical datasets. In potential field gravity data, linear features may be interpreted as spatial discontinuities in bedrock density. They correspond to subsurface geological faults and density contrasts that may also be lithological rock unit boundaries (Pilkington & Keating 2009, Aydogan 2011). Less frequently, the detection of geologic lineaments may be based on radiometric (Debeglia et al. 2006) and electromagnetic data (Paananen et al. 2013). However, the effects of alteration and weathering on the concentration or dispersion of radiometric elements, or in enhancing or reducing conductivity, can lead to ambiguous interpretations, i.e. lineaments may be observed as maximum or minimum anomalies.

The effective survey depth range and availability make aeromagnetic data the most commonly used information source for lineament detection. Hence, interpretation tools for magnetic datasets in structural studies have been quite thoroughly assessed and developed. The detection of crustal weaknesses and fractures from magnetic data is based on the fact that they can be observed as minimum magnetic lineaments caused by the magnetic susceptibility contrast between the fractures and host rock (e.g., Airo & Wennerström 2010). Minimum anomalies may be a result of fluids affecting the mineral stability of magnetite and ferromagnesian minerals by partial destruction of the magnetite crystal structure, or the removal of magnetite during crustal deformation (Mertanen et al. 2008). In addition, in weathering-induced clay alteration of deep brittle fractures zones, magnetite alters into iron oxides and hydroxides (Henkel & Guzmán 1977, Grant 1984, Olesen et al. 2006). Recognition of these negative magnetic anomalies in fracture zones has been hindered in Finland by glacial processes, e.g. the removal of *in situ* weathered sapprolite and exposition of the less altered bedrock. Simultaneously, these topographic depressions might be filled with exogenic sediments. Thick overburden attenuates the magnetic field, which especially affects the detection of weakness zones. In addition, magnetic data may also be used to detect other geological linear structures by using filtering techniques based on derivatives (Pilkington & Keating 2009). In addition to minimum anomalies, magnetic lineaments can be outlined as maximum anomalies (e.g., dykes) or simply as an interface between two lithological units.

Faults in magnetic data can be observed as discontinuities and displacements (i.e., truncations and offsets) of magnetic or non-magnetic bodies. In Finland, the current interpretation of the structures is merely based on linking together these features in the magnetic data. Connecting the linear breaks in magnetic data that line up as a structure is a common practice in structural mapping (e.g., Airo & Leväniemi 2008). Similarly, DEMs and aerial photographs are utilized, and the lineament detection is complemented with field observations, geological expertise, and confidence in interpretation to provide a structural interpretation including a classification of the structures according to their origin and geometry. Rarely are near complete interpretation schemes reported, such as presented by Paananen (2013) for nuclear waste

deposits studies and Airo & Leväniemi (2008) for gold exploration.

Lineaments are detected from data either visually or with pattern recognition techniques, which are numerous and variable in success (see section 2). Object-based image analysis (OBIA) is a semi-automated image processing technique. It differs from other image processing approaches in that the raster data are first segmented into homogeneous regions of pixels, i.e., objects, and classification takes place after utilizing not only the pixel data values but also the shape and context information of an object (Blaschke et al. 2008). Thus far, a few authors have applied the OBIA framework in lineament analysis. Sukumar et al. (2014) claimed that linear filtering and object-based classification guarantee a high degree of accuracy for a lineament mapping project based on high resolution optical imagery. Marpu et al. (2008) also tested OBIA methods on SAR, Mavranza & Argialas (2008) on Landsat data, and Rutzinger et al. (2007) on LiDAR DEM quite successfully. Argialas & Mavrantza (2008) used object-based image processing for the knowledge-based categorization of line features derived by the EDISON algorithm from Landsat data, i.e. line features were named as structural faults, structural joints and non-faults based on their position in the lithological map. Stumpf et al. (2013) also used the object-oriented approach to improve the accuracy of landslide linear fissure detection from high resolution visible and LiDAR data. Based on these reports, it appears that OBIA is quite feasible if the features can be clearly visualized from the raw data or its transformations.

The purpose of this paper is to introduce an OBIA approach in lineament detection. The objective is to test an OBIA pattern recognition approach in the detection of TDR minimum ‘worms’ from airborne magnetic data. In this paper, we consider ‘worming’ in a broader sense, including the detection of edges in potential field data produced with two techniques: a multiscale wavelet edge approach (Hornby et al. 1999) or curvature analysis (Phillips et al. 2007). Originally, ‘worms’ were only considered as a product of the multiscale wavelet edge approach (Hornby et al. 1999). This work compares the OBIA result to ‘worming’ with curvature analysis by Phillips et al. (2007). An image-processing algorithm for ‘worming’ is developed with Cognitive Network Language (CNL) in eCognition software (Trimble Geospatial, Munich, Germany). The visual interpretation results

of the magnetic data and high resolution DEM acquired through laser scanning are also presented and the strengths and weaknesses of visual vs. pattern recognition techniques are discussed. Ultimately, a broader objective is to develop computer-assisted knowledge-based lineament detection from a variety of data sources complemented with expert knowledge and field observations to assist in structural mapping, lithological mapping and mineral potential mapping. The intent is not to produce a comprehensive expert geological

interpretation of lineament types or their origin, but to review a set of tools for the preinterpretation of topographic and geophysical data for structural geologists to draw their attention to potential linear features and to utilize the data to their full potential. Thus, the mechanical work of digitizing would be minimized and the focus would be on geological interpretation. It would be meaningful to use these methods at the beginning of a project so that field campaigns can be targeted at detecting their reliability and accuracy.

## REVIEW OF VISUAL VS. SEMI-AUTOMATIC LINEAMENT DETECTION

In lineament detection, based on image interpretation only, the separation of non-geological lines and alignments such as roads, water courses and fissures from geologic lineaments is troublesome. Traditionally, the interpretation of raster data has been conducted visually by a trained geologist or geophysicist. The advantage of human interpretation is the ability to scan large areas quickly and recognize discontinuous linear patterns such as truncations and offsets. However, poor reproducibility between different operators and a lack of proper geological understanding of the areas causing random distribution of lines are the disadvantages of traditional interpretation, although this can be enhanced by using several independent interpreters (Sander et al. 1997, Sander 2007).

Computers, on the other hand, excel in optimization, detailed delineation and repetition. In particular, interpretation for monitoring purposes is more accurate with pattern recognition because of the systematics that can be incorporated into an algorithm (Quackenbush 2004). The objectivity and reproducibility of computer-based pattern recognition is the driving force behind the development of computer-assisted structural analysis. However, pattern recognition techniques do not produce identical results to manual interpretation, but as both techniques detect different linear patterns they should be considered complementary rather than exclusive. Several authors also claim that the semi-/automatic pattern recognition methods produce more structures compared to human interpretation (Abdullah et al. 2013), implying that image processing might be better at enhancing weak subtle linear features, especially in magnetic

data, which might be equally significant compared to stronger features.

Line extraction is a highly researched area of pattern recognition that is also common in blood vessel segmentation (Kirbas & Queck 2003), road extraction (Quackenbush 2004) and watercourse extraction (Dillabaugh et al. 2002). There is a diversity of pattern recognition approaches to produce vectorized representations of lineaments from gridded data with image processing methods. In general, regardless of the data, semi-automated lineament detection procedures have five steps: preprocessing, edge detection, edge tracking, edge linking and vectorization. With the potential field magnetic and gravity data, the currently most common procedure is to utilize a variety of derivatives as edge enhancement filters (Fairhead & Williams 2006, Pilkington & Keating 2009), whereas in optical and topographic lineament detection the methodology and the success rate of the approaches is more diverse, including a variety of spatial (e.g., Sobel, Prewitt, LOG, Canny) and frequency edge detection filters (e.g., Gaussian, Butterworth, see Quackenbush 2004, Rahnama & Gloaguen 2014). Once edge pixels are identified with the filters, a common procedure is then mathematical morphology, including dilation, erosion or curve thinning (see e.g. Beauchemin & Lamontagne 2011, Rahnama & Gloaguen 2014). Edge tracing and following into vector line features is then finally performed, e.g. with Hough transformation (e.g. Fitton & Cox 1998), segment tracing (Koike et al. 1995), snakes (Gruen & Li 1997) or 'worming' (Hornby et al. 1999, Phillips et al. 2007). A large number of different algorithms are available for all of these stages of image processing (Quack-

enbush 2004, Sukumar et al. 2014), a few of which are mentioned here. Comparison of the pattern recognition approaches is impossible, as each approach is designed and optimized for the available

data. Most methods are not truly objective but rather semi-automated, because the techniques require user input to be adapted for different image types, quality and environmental settings.

## GEOLOGY AND TECTONIC SETTING OF THE ENONTEKIÖ STUDY AREA

The bedrock of the Enontekiö study area (Fig. 1) consists of a western domain of mainly Archaean metasedimentary and metavolcanic rocks, juxtaposed against Palaeoproterozoic metasedimentary and metavolcanic rocks in the central and eastern parts of the region. The transition is complex and windows of Archaean basement are exposed at the surface in a number of structural culminations within the Palaeoproterozoic domain. In addition, intrusive mafic rocks are present, such as gabbros, most notably the 2.4 Ga Tsohkoarvi complex, and swarms of diabase dykes with a characteris-

tic NW–SE trend; such mafic rock compositions also generally tend to be geophysically responsive, and are typically associated with positive magnetic anomalies (Bedrock of Finland – DigiKP, Karinen et al. 2015). A mapping project to improve understanding of the bedrock geology and stratigraphy is under way (Jukka Konnunaho and Tuomo Manninen, personal communication, August 2014).

Structural mapping for lineaments, e.g. minor faults and fractures, in the GTK digital bedrock database, DigiKP, is illustrated in Figure 2, superimposed upon the airborne magnetic anomaly

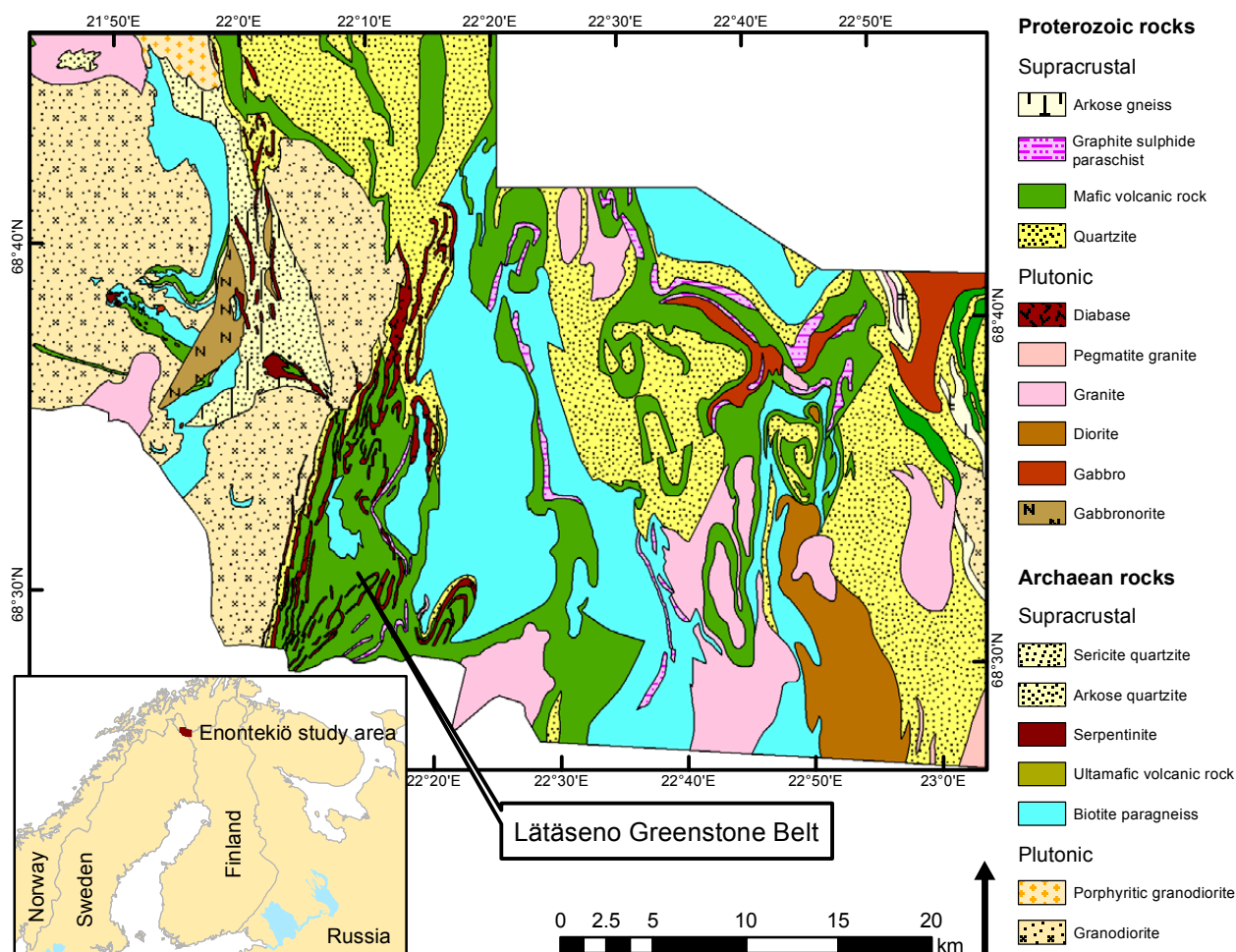


Fig. 1. Lithology of the Enontekiö study area. Edited from the digital bedrock database: Bedrock map (Bedrock of Finland – DigiKP). Geographic coordinates: WGS84. Figure: Maarit Middleton, GTK.

map. Structural interpretation was mainly based on visual interpretation of the airborne magnetic data and verification of the lineaments through field observations. Topographic lineaments were also interpreted from the 10 m pixel size DEM by the National Land Survey of Finland (NLS) and from aerial photographs with 0.5-m resolution also provided by the NLS (Jukka Konnunaho, personal communication, October 2014). Some of these linear features appear to have crustal-scale dimensions and significance. For example, there is a prominent NNE–SSW-oriented feature that can be traced across the entire study area from Sweden to Norway (see Bergman et al. 2001), known as the Karesuando-Arjeplog ductile deformation zone (KADZ). This feature is evident in the magnetic image in Figure 2 (as well as in the geological map in Fig. 1), and coincides in part with the boundary between Archaean basement granitoids to the west and the Lätäseno Greenstone Belt rocks to the east. However, alternative interpretations are possible, assigning greater significance to the N–S-trending feature on the eastern flank of the Lätäseno Greenstone Belt (Fig. 1) referred to as the Lätäseno Shear Zone (LSZ) by Karinen et al. (2015). Such uncertainty and ambiguity is inherent in this type of study, resulting from three factors in particular:

- 1) Self-referencing or auto-correlation, where for example, in poorly exposed terrain, geological boundaries are drawn on the basis of geophysical anomalies. Later interpretations may then make erroneous assumptions concerning the independent nature of separate datasets or layers.
- 2) While many natural phenomena and structures are self-affine, with fractal repetition across a range of scales, there may still be difficulties in verifying and correlating large-scale features discerned in remote analysis with structures observed at the outcrop scale.
- 3) A geophysical or geochemical anomaly or measurement essentially represents the sum-

mation of all events and processes that have affected the material properties and composition of a given rock volume or planar structural feature. Therefore, the challenge is how to extract an event history from visual analysis, or to exclude unlikely interpretations. In areas where the bedrock is well exposed and easily accessible, there is a greater opportunity for determining the sequence of overprinting events and the geometry and kinematic history of structures using field-based constraints.

The KAZD illustrates these issues, depending on how we interpret its development over time, and as an example of how a particular structure may be reactivated during different events. This feature, which separates older Archaean basement rocks in the west from the predominantly younger sediments and volcanic of the Lätäseno Greenstone Belt, may be explained in several ways. Firstly, it might have been initiated early, as an extensional growth fault accommodating the accumulation of sediments and volcanics in a subsiding rift basin. In this case, we could explain differences in the nature and thickness of rock units (and hence the geophysical signature) across the deformation zone as being inherited from early rifting events. Alternatively, the deformation zone may have developed during compressive deformation, perhaps at the boundary between two rock units having contrasting mechanical behaviour. In this case, we could offer several plausible interpretations, including 1) a low-angle thrust, emplacing one terrain or block over another, thus explaining the abrupt change in nature of rock units, or 2) a steeply dipping shear zone with combined strike-slip and vertical displacement, which would cause differential lateral displacement or erosion of one side of the deformation zone with respect to the other (again resulting in geophysical contrasts across the zone).

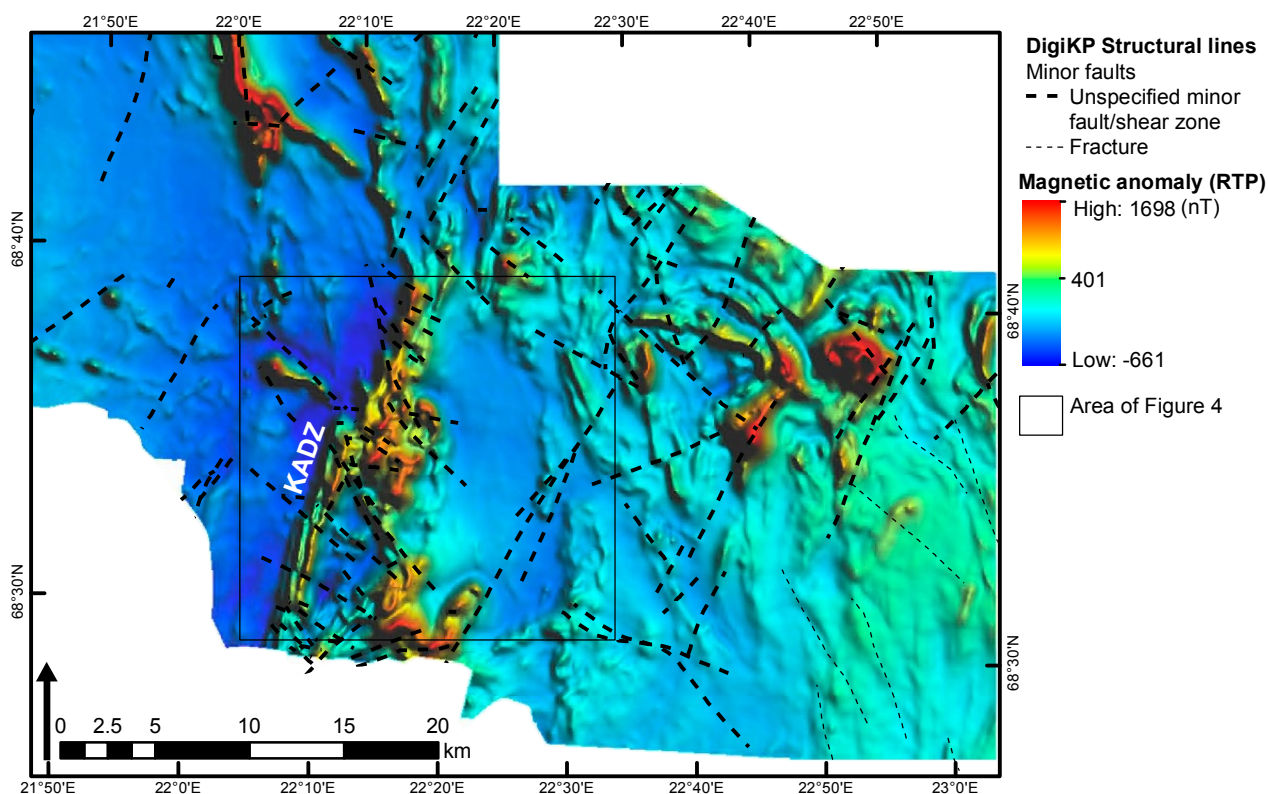


Fig. 2. Colour-shaded magnetic IGRF-65 anomaly map, reduced to pole (RTP). Structural lines from the digital bedrock database: Bedrock of Finland – DigiKP. Karesuando-Arjeplog deformation zone marked as KADZ. Geographic coordinates: WGS84. Figure: Maarit Middleton, GTK.

## DATASETS AND PREPROCESSING

### Airborne magnetics and LiDAR

Airborne magnetic data were acquired in a nationwide airborne geophysical programme of the Geological Survey of Finland (GTK). Magnetic measurements were carried out simultaneously with frequency-domain electromagnetic and radiometric measurements with 200 m line spacing at 30–40 m nominal altitude. Hautaniemi et al. (2005) and Korhonen (2005) provided descriptions of the measurement systems and data processing. The Enontekiö study area consists of three flight areas, two of which were flown in 1983 and one in 2002 all in an E–W direction (see Torppa et al. 2015). In 2002, the magnetic field was sampled 10 times/second and acquired with a caesium magnetometer flown in a fixed-wing aircraft. The 1983 data were acquired with a registration rate of 2 times/second using a proton magnetometer. The measured total magnetic induction (TMI) was subjected to preprocessing (Fig. 3). The International Geomagnetic Reference Field (IGRF)

was subtracted from the TMI and reduction to the northern pole (RTP) was carried out in order to model the field if measured at the North Pole and thereby to improve the geometric response of the anomalies. The RTP magnetic anomaly data were further continued upward to 200 m to remove noise and to emphasize regional-scale features (Fig. 3, Fig. 4a).

Airborne Light Detection And Ranging (LiDAR) is an active technique based on the sending of a high-energy monochromatic light beam from an airborne platform and measuring the travelling time of that beam in order to determine the distance to a target. The pulse is first reflected from vegetated surfaces (e.g. first-return canopy), but some energy continues and finally reflects from near ground (i.e. last-return ground surface). The last returning pulses of the point cloud are classified as ground returns and are utilized for creating a DEM. The airborne LiDAR data was acquired for

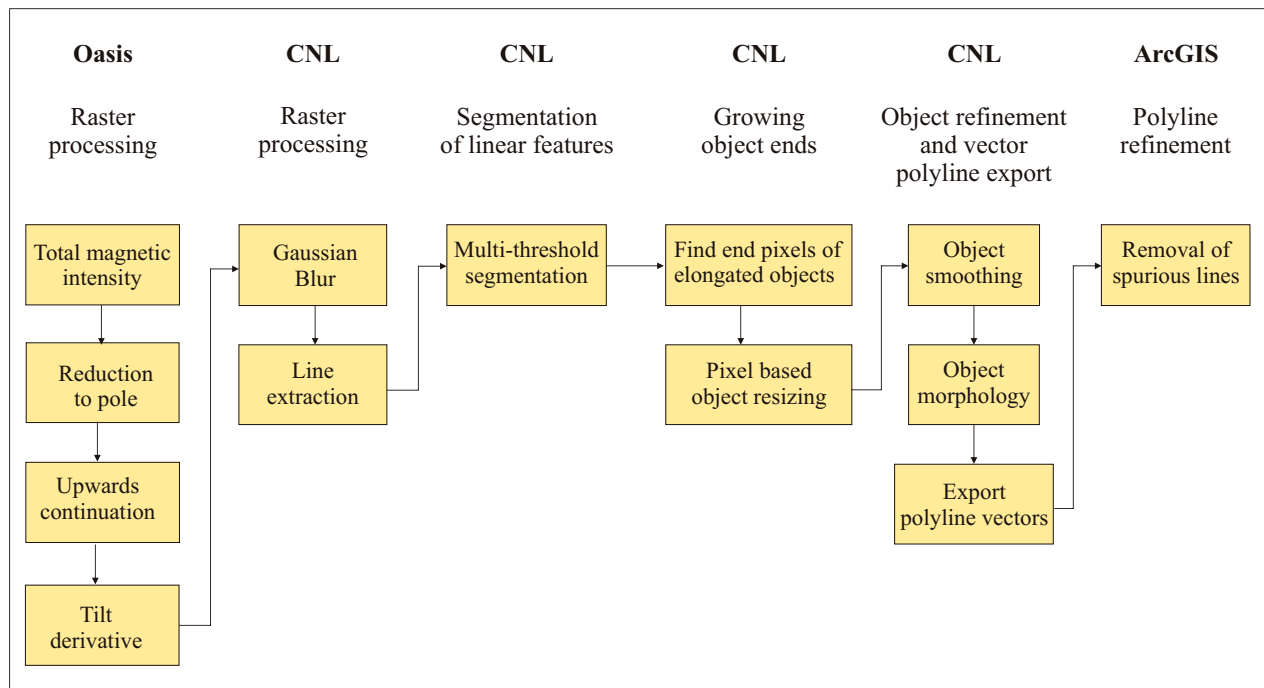


Fig. 3. Processing chain of gridded aeromagnetic data including preprocessing in Oasis, Cognitive Network Language image processing steps of the Object-Based Lineament Detection algorithm in eCognition, and ArcGIS refinement process of created polyline ‘worms’. Figure: Maarit Middleton and Viena Arvola, GTK.

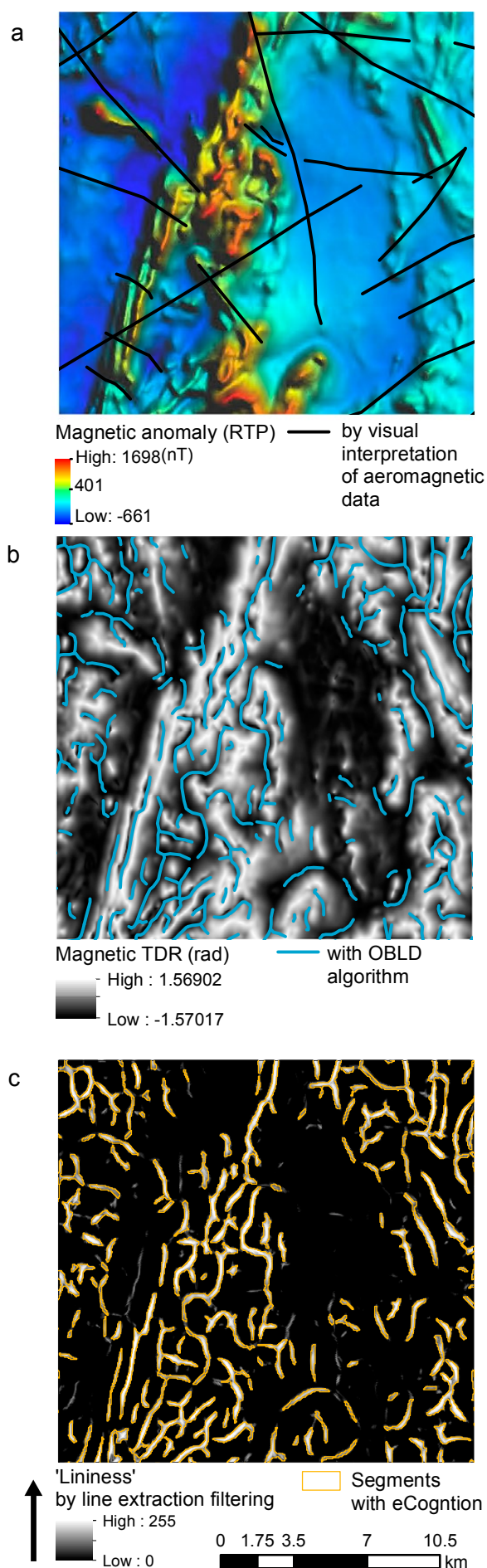
the NLS by Blom Geomatics with an Airborne Laser Terrain Mapper Gemini laser scanner (Optech Inc., Vaughan, Canada) from a flight altitude of 2100 m, with a scanning frequency of 37 Hz and a pulse frequency of 70 kHz, resulting in an average point density of 0.76 points/m<sup>2</sup>. The southern half of study area was flown on the 5 June 2013, and the northern half between 22 and 24 July 2013. A 6-km-wide strip on the eastern side of the study area was already flown on 16 September 2012, in a NE direction with a Leica ALS50-II laser scanner (Leica Geosystems, St. Gallen, Switzerland)

using a slightly higher point density (2410 m, 43.5 Hz, 108.6 MHz, 1.06 points/m<sup>2</sup>, respectively). The canopy obscurrence of the pulse in the study area is relatively insignificant because the tree coverage is sparse, especially in the northern part of the study area, which has even fewer mountain birch trees compared to the southern part. The vertical ground resolution was verified against the VRS-GPS measurements, producing a root mean squared error of 0.009–0.06 m. The ground pulses were extracted and interpolated to a 2 x 2 m DEM.

### Preprocessing filters

To enhance the structural features of the magnetic data, the tilt derivative (TDR, Fig. 3, Fig. 4b) available in Oasis (Geosoft Inc., Toronto, Canada) was applied. The TDR is the arctangent of the ratio of a vertical to a combined horizontal derivative (Miller & Singh 1994, Verduzco et al. 2004). With regards to the magnetic data, it was calculated from upward-continued (200 m) RTP-corrected magnetic anomaly data. The TDR was used because it equalizes the amplitude of anomalies (see Smith & Clark 2005) and thus emphasizes weak magnetic

features. Amplitude values are restricted to values between -90° and 90° (i.e.  $\pm \pi/2$ ). In the magnetic data, the continuous elongated TDR minima may be related to weakness zones in the bedrock, which could be shear, fault or thrust zones (Lahti & Karinen 2010, Airo & Leväniemi 2012). In this study, we also applied TDR to the LiDAR-acquired DEM to enhance the visual appearance of the linear geomorphological features (see Sutinen et al. 2014). The TDR equalizes the amplitude of anomalies and thus emphasizes the geomorphological



features. The zero contours are located close to the source contact, e.g. at the base of the geomorphological feature.

The visual lineament interpretation of the magnetic and the LiDAR DEM data was mainly based on the TDR. The TDR was also applied to magnetic data using the semi-automatic 'worming' technique. For the object-based image analysis of lineaments from the magnetic data, additional filtering was applied. In eCognition, the TDR was convolution filtered with a Gaussian smoothing filter called Gaussian Blur (eCognition Reference Book, v. 9.0.1, Fig. 3). This filter replaces each pixel value with the average of the square area of a matrix centred on the pixel. The purpose was to remove noise and unnecessary detail, which was successfully accomplished using a small window size of 3 x 3 pixels. Finally, a line extraction algorithm was applied (eCognition Reference Book, v. 9.0.1, Fig. 3, Fig. 4 c). The line extraction filter is a rectangular filtering approach in eCognition. The line extraction kernel consists of 3 substripes: a centre stripe and 2 border stripes, which are defined with algorithm parameters such as the line length (used parameter: 15), line width (1, 3, 5, 7, 9, and 12 pixels), border width (2) and line direction (0–179 at 5-degree intervals). The filter uses mean values and standard deviations of the pixels in each of the stripes to calculate the likelihood of forming a line. An "ideal" line in this respect has similar border stripes on both sides and high contrast between centre stripes and border stripes. The calculation is controlled by the parameters minimal pixel variance (variance of the input layer) and minimum mean difference (detects dark lines). 'Minimal pixel variance' specifies a threshold of variance to compare the stripes, and the 'minimum mean difference' defines whether dark or bright lines are detected. The output is a raster

Fig. 4. Magnetic anomaly map and visually interpreted structural lines from airborne magnetic data reduced to pole (RTP, 4a). Tilt derivative (TDR) of the magnetic anomaly map overlaid by TDR minimum 'worms' using the Object-Based Lineament Detection (OBLD) algorithm (4b). Result of the line extraction filter, i.e. 'lininess', calculated from TDR overlaid by objects from Multi-threshold segmentation in eCognition (4c). The final 'worms', i.e. vector lines, in 3b were created from the objects in 4c. The area of the figures is drawn on Figure 2. Figure: Maarit Middleton, GTK.

of 'lineness', i.e. similarity of pixels in the neighbourhood of a pixel compared to a straight line. A separate raster was calculated for each direction (0–179 at 5-degree intervals) defined with 'line direction parameter'. These rasters were summed

together and scaled to an 8-bit image to produce a single output raster that includes 'lineness' in all directions, including six widths (Fig. 4c), adapting a toolset 'Line Extraction Sample Rule Set' available from the eCognition Community webpages.

## LINEAMENT DETECTION METHODS

### Semi-automated 'worming' techniques

#### Lineament detection algorithm in Cognitive Network Language

An Object-Based Lineament Detection (OBLD) algorithm was developed with the CNL to detect the continuous minima ('worms') of TDR derived from the aeromagnetic data (see Fig. 3). The key for the successful recognition of the lineaments with eCognition was the line extraction algorithm described in section 4.2. The highest values of the 'lineness' raster (>11) were first segmented with a 'Multi-threshold segmentation' algorithm (Fig. 4c), which splits the image object domain and classifies resulting image objects based on a defined pixel value threshold. Small segments (<6 pixels) were then removed and some cleaning was carried out. Secondly, more subtle features attached to the end of the original line segments were found and merged into the line segments. This was done by using the hierarchical object levels available in

eCognition. The original line objects were assigned as super-objects, and 'Chessboard segmentation' was applied to the sub-object level to assign each pixel as an object. 'Chess-board segmentation' divides the data into equal-sized square objects. An object feature called 'Is end of super object' was applied to these objects to find the end objects of the linear segments. These end objects were then copied on the super-object level. In order to grow the end pixels meaningfully only within linear features, we applied an algorithm called 'Pixel-based object resizing'. The growing was limited to raster values of 'lineness' less than 6. In the third stage, refinement of the line objects was performed. The objects were smoothed and close objects were attached together. Finally, the main lines and skeletons of these polygons were exported as line vectors. Unnecessary short branches were detected in the widest parts of the objects. Therefore, the vector skeletons were exported into GIS for final cleaning.

#### 'Worming' by curvature analysis

Phillips et al. (2007) introduced the use of curvature analysis for gridded potential field data. The method first fits a local quadratic function to a window of 3 x 3 data points and then the 'critical point', i.e. position on a ridge that lies closest to the centre of the window, is established. If the critical point was far from the window centre it was rejected. The eigenvalues and eigenvectors of the curvature matrix associated with a quadratic surface can be used to locate the sources and estimate their depths and strikes. The sign of the eigenvalues of the curvature matrix indicated whether a ridge or a trough was present. The plan curvature method produces continuous ridges and valleys and appears to be a very effective method for the interpretation of linear features and especially

weak features in the magnetic data (Hanna Leväniemi, personal communication, October 2014). Geosoft eXecutables, GX Tool, developed by the USGS (Phillips et al. 2007) and available in Oasis was applied in order to locate local minima of the TDR derived from the aeromagnetic data. Discrete source point locations estimated with the GX Tool were connected into lines that follow faults based on the maximum distance between points (100 m) and maximum strike deviation (30 degrees). The points were connected with a 'Connect points' tool also implemented in Oasis by Leväniemi (2011), adapting the code suggested by Phillips (2007). Finally, lines shorter than 800 m were removed to get rid of the small-scale variance that is not geologically significant on the regional scale.

## Visual lineament interpretation

In visual interpretation, long straight continuous features were digitized in a GIS environment. In this study, the visual interpretation was carried out separately for aeromagnetic data and DEM data. Magnetic lineaments were analysed on the basis of upward-continued (200 m) magnetic data. Lineaments forming long elongated anomalies were outlined using magnetic anomaly data illustrated with varying colouring and shading techniques. The interpretation of the more subtle lineaments was carried out using TDR data. Topographic lineaments were interpreted based on the TDR calculated from LiDAR DEM data. We delineated both the topographic valleys (i.e., deformation zones) and also the long continuous scarps (i.e., vertical faults, lithological contacts). In topographical interpretation, glacial lineations with a prevailing direction of 15–40 degrees (NE) were avoided. They appear as subtle elongated flutings cross-cutting the more pronounced bedrock-induced features.

Structural interpretations of the data could not be checked in the field, which means that considerable uncertainty and ambiguity remains. There are simple principles for determining event history, using qualitative and subjective analysis based on a combination of experience and analogy. The most obvious principle is searching for examples where displacements of one trend by another are

recognizable, and preferably demonstrable using more than a single anomaly. It is also important to be aware of the risk of perception bias, with a tendency to link short linear sub-parallel features into a single trend. This particularly applies to the NW–SE trend in the present case, with the more prominent, discrete KADZ giving the impression, probably erroneous, of being superimposed upon, and truncating the NW–SE trends. The next important pattern to assess in comparing qualitative, experience-based assessment against the results of semi-automated pattern recognition result was where there is a great diversity of trends. Could these all be related to complex geometrical folding or disruption of a single, continuous layer, or do they represent a myriad of randomly oriented, unrelated and superimposed structures and events? For example, it is more intuitively obvious to interpret the accurate features in the eastern part of Figure 4 as interference patterns due to complex folding of a discrete stratigraphic package. In addition to truncation relationships and fold patterns, hydrothermal processes along fracture zones may induce mineralogical changes that enhance or reduce magnetic susceptibility, or the radiometric response. Such changes can be very useful in deducing the sequence of structural events.

## RESULTS AND DISCUSSION

The curvature analysis with GX Tool software produced a very detailed interpretation of the local linear features and also of the subtle aeromagnetic signatures (Fig. 5). The question is whether all of the identified subtle features are relevant for lineament interpretation. Visual comparison with magnetic and DEM data reveals that some of these ‘worms’ are related to lithological boundaries, but the majority of them indicate structures within the lithological units. The TDR also receives long continuous local minima on the flanks of the continuous magnetic lithological bodies (see Fairhead & Williams 2006). This can be well visualized, e.g. on the eastern edge of the Lätäseno valley, where gabbros can be seen as the maximum anomalies of the magnetic data (see Fig. 4b). Therefore, it has to be noted that not all of the structures are related

to bedrock weakness zones, but rather to other gradients in magnetic data that may be lithological boundaries, but also possibly weakness zones. The true lithological source of the features in the Enontekiö area remains uncertain without field verification.

Although ‘worms’ are associated with geological structures, only a few studies have actually shown their spatial relationship with mineralizations. Gravity ‘worms’, in particular, have been found to be spatially correlated with epigenetic gold occurrences (Bierlein et al. 2006, Lahti et al. 2014). There may be at least two principal reasons for this. Firstly, lateral density gradients may correlate with significant crustal boundaries, with a first order correlation between large-scale tectonic processes, metamorphic gradients and rock permeability and

structure, all of which contribute to the efficiency of metal transport and deposition. Secondly, and often at a more local scale, the contacts between intrusive bodies and country rocks may coincide with both density contrasts and magnetic anomalies. In some cases, intrusions may provide heat sources for driving hydrothermal convection and metal transport, but more typically the mechanical contrast between massive intrusive rocks and more anisotropic country rock units will influence rock strength, failure and permeability and thereby influence the transport and focusing of hydrothermal fluids.

The strength of the 'worming' technique using curvature analysis is the ability to detect very subtle linear features that are continuous. It may also be used to detect magnetic maximum anomalies. Even though it fails to detect horizontally discontinuous breaks, it can be seen as another visualization technique to highlight elongated patterns in data. In visual interpretation, discontinuous lineaments, i.e. linear truncations and offsets, are often linked to long continuous features. 'Worming' might also help in detecting these features, as

illustrated in the SW corner of the maps in Figure 4. The 'worms' in Figure 4b are offset by a faulting and can be visually interpreted as in Figure 4a.

The results of the OBLD algorithm are presented in Figure 6 over the curvature analysis also presented in Figure 5. The OBLD algorithm produces results that are very similar to the curvature analysis, although the pattern recognition approaches are different. Both methods rely on finding local elongated minima of the TDR raster. However, the heart of OBLD is the line extraction filtering that enhances the linear features in the convolution filtered TDR raster. The 'lineness' raster is then thresholded into segments representing the lineaments. By contrast, curvature analysis produces a point file where each point represents a local TDR minimum. These points are then connected into vector lines with the connect points tools. The OBLD algorithm fails to detect the most subtle features, the ones lying in wide 'valleys' of the TDR raster, such as can be seen in the centre of Figure 6. The OBLD algorithm can be downloaded from the eCognition Community webpages (<http://www.ecognition.com/community>).

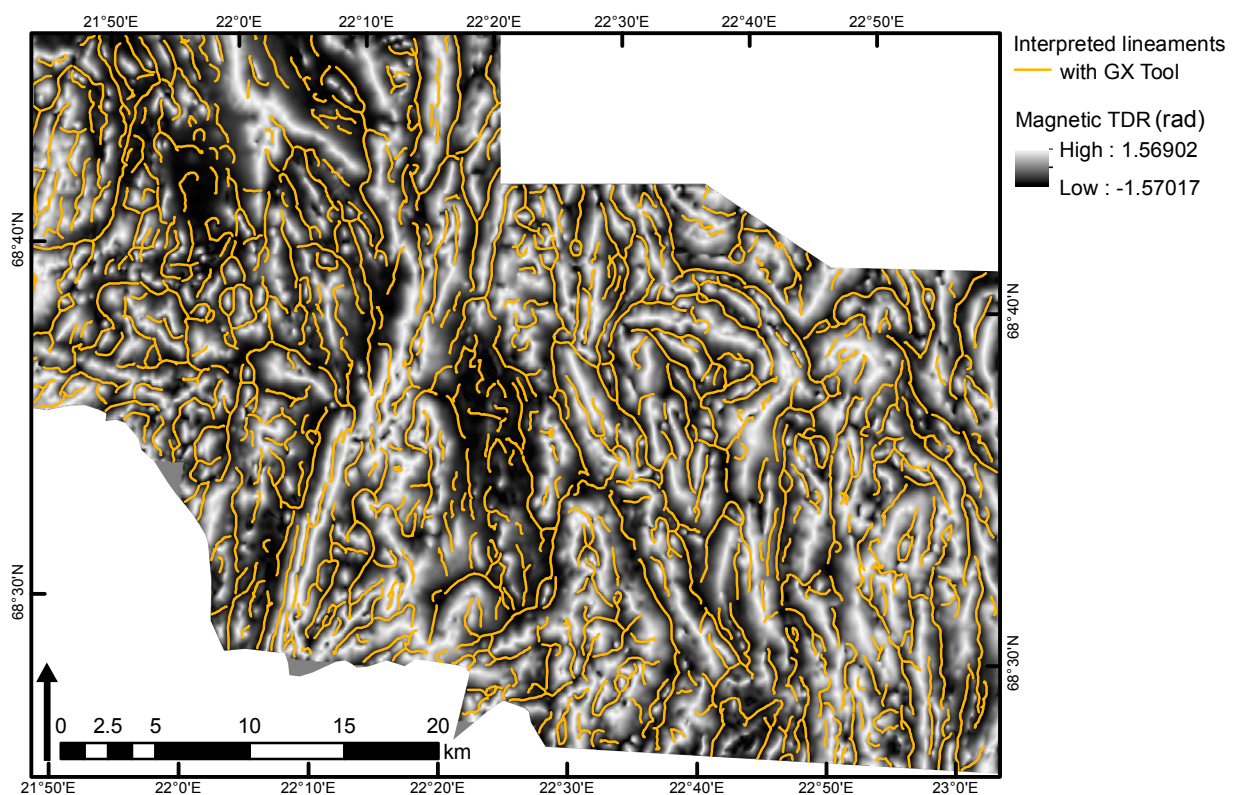


Fig. 5. Semi-automatic interpretation of linear features with curvature analysis in the GX Tool package (Phillips 2007). The local TDR minima depicting possible weakness zones are well detected with the curvature analysis. Lineaments are overlain on the tilt derivative (TDR) of airborne total magnetic induction reduced to pole. Geographic coordinate system: WGS84. Figure: Maarit Middleton and Eija Hyvönen, GTK.

An advantage of CNL is that it offers a user-friendly graphical user interface (GUI) for image processing and a versatile image interpretation tool set for lineament detection. It is a flexible development environment for geological interpretation. The downside is that it presents a steep learning curve and requires a commitment to developing a flexible algorithm in the beginning. Once a rule-based algorithm is completed, it can easily be applied to other places once identical data preprocessing is performed. The CNL algorithm can also be set up in an end-user-friendly 'architect' solution that simplifies the GUI but allows adjustment of the parameters specific to an area under study. Previously, little work in geological lineament detection has been conducted with CNL. The created OBLD algorithm can be used similarly to other 'worming' methods, e.g. it can be applied to different levels of upward continuation of the potential field to detect the short and long wavelength gradient minima and to visualize them in 3D.

The visual interpretation of the airborne magnetic RTP and its TDR combined is presented

in Figure 7. Compared to the interpretation presented in Figure 2, the results are quite different. In Figure 2, the interpretation was based on basic aeromagnetic data with minor geological observations. The interpretation in Figure 7 is only based on aeromagnetic data without any geological observations. In addition, the interpretation of Figure 7 was mainly carried out using TDR data, and thus the number of lineaments located in areas of weak magnetic anomalies is higher. Visual interpretation is a subjective result of interpretation and it depends on the data, data processing, the scale of interpretation, the experience of the interpreter, and the amount of available field data. Therefore, the interpretation results vary greatly. During the visual interpretation, it was realized that computer automatization of this type of lineament interpretation would be very complicated, possibly impossible. This is especially true for the OBIA approach, which requires clear visualization of the features in the data.

In the study area, two sets of lineaments were detected, oriented in NE-SW and NW-SE di-

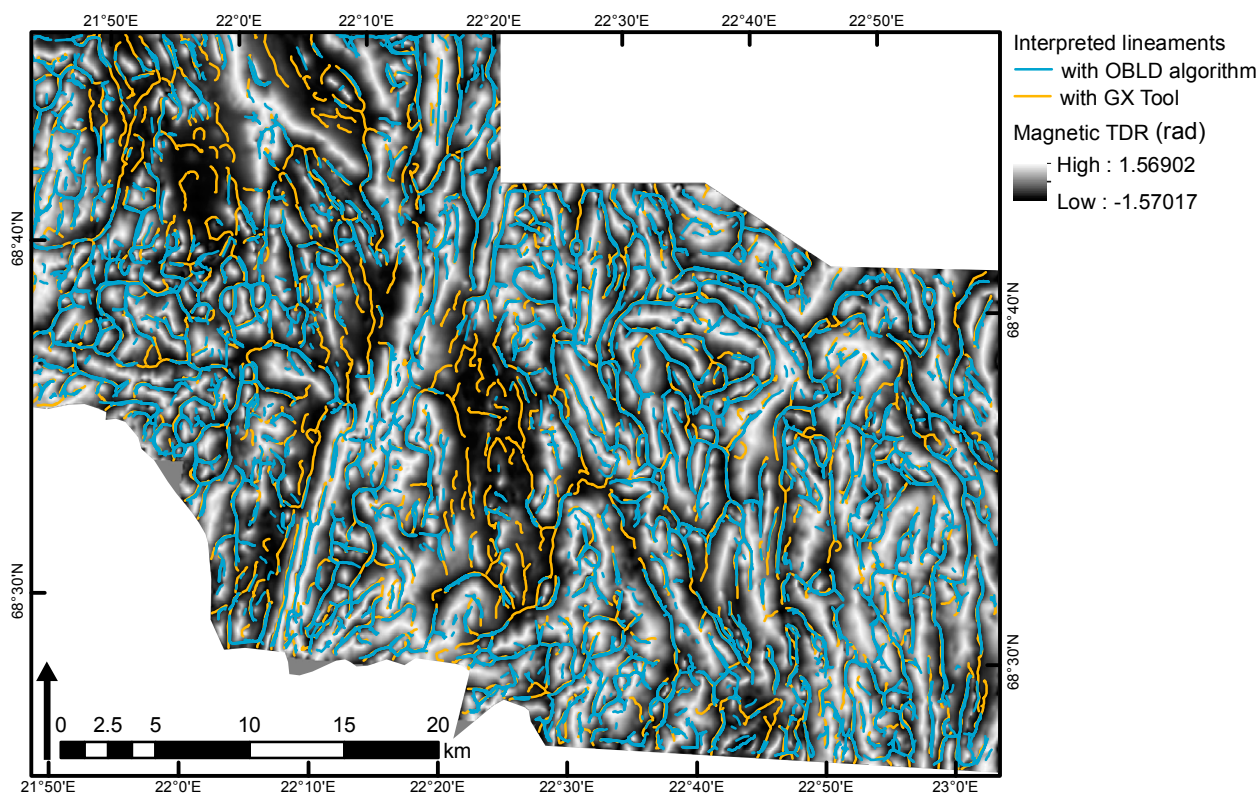


Fig. 6. Two 'worming' methods applied to interpret the same data: the tilt derivative (TDR) of aeromagnetic data reduced to pole (RTP). The developed Object-Based Lineament Detection (OBLD) algorithm in eCognition software fails to detect the weakest local TDR minima in the data, e.g. in the centre of the study area. Therefore, interpreted lineaments are also less continuous compared to those created by curvature analysis with the GX tool and Connect points tool in Oasis. Geographic coordinate system: WGS84. Figure: Maarit Middleton, GTK.

rections. Their mutual cross-cutting relationship remains ambiguous. The NNE–SSW-trending KADZ separates two geological domains whose internal features and complexity differ significantly from one another. There are no constraints concerning the potential displacement along this deformation zone, for which three plausible interpretations may be offered. Firstly, it may simply be a modified unconformity between Archaean and Proterozoic rocks, Secondly, there could be significant thrusting or strike-slip deformation subparallel to the zone, which may have brought two different terrains together. Thirdly, vertical movements have exhumed and eroded different crustal levels, with different rock types now exposed on either side of the deformation zone. Similarly, ambiguity in interpretation remains with respect to the NW-trending anomalies and edge enhancement features; since some of the NW-trending features cause minor offsets of the KADZ, it is reasonable to infer that they are younger. There are also other NW-trending features that could terminate against the KADZ. This does not in itself prove that the

KADZ truncates older NW-trending features, as changes in material properties across the KADZ could also explain their absence or deflection. Indeed, it is possible that some of the NW-trending magnetic features might relate to the Palaeozoic Caledonian orogen, as well as representing Palaeoproterozoic dyke swarms, which characteristically have NW trends in the Fennoscandian Shield. The abundant NE-trending features on both sides of the KADZ might also relate to a brittle crustal response by the Fennoscandian lithosphere during the Caledonian Orogeny, although the emplacement of granites within the 1.8-Ga Trans-Scandinavian Batholiths might also have generated such fracture trends.

The visual interpretation of the linear structures from the LiDAR-acquired DEM is presented in Figure 8. Compared to the visual interpretation of the magnetic data (Fig. 7), several additional topographic lineaments (Fig. 8) were detected. The topographical lineaments follow the same orientation, i.e. NE–SW and NW–SE, and location as the magnetic lineaments (Fig. 7, Fig. 8). Topographic

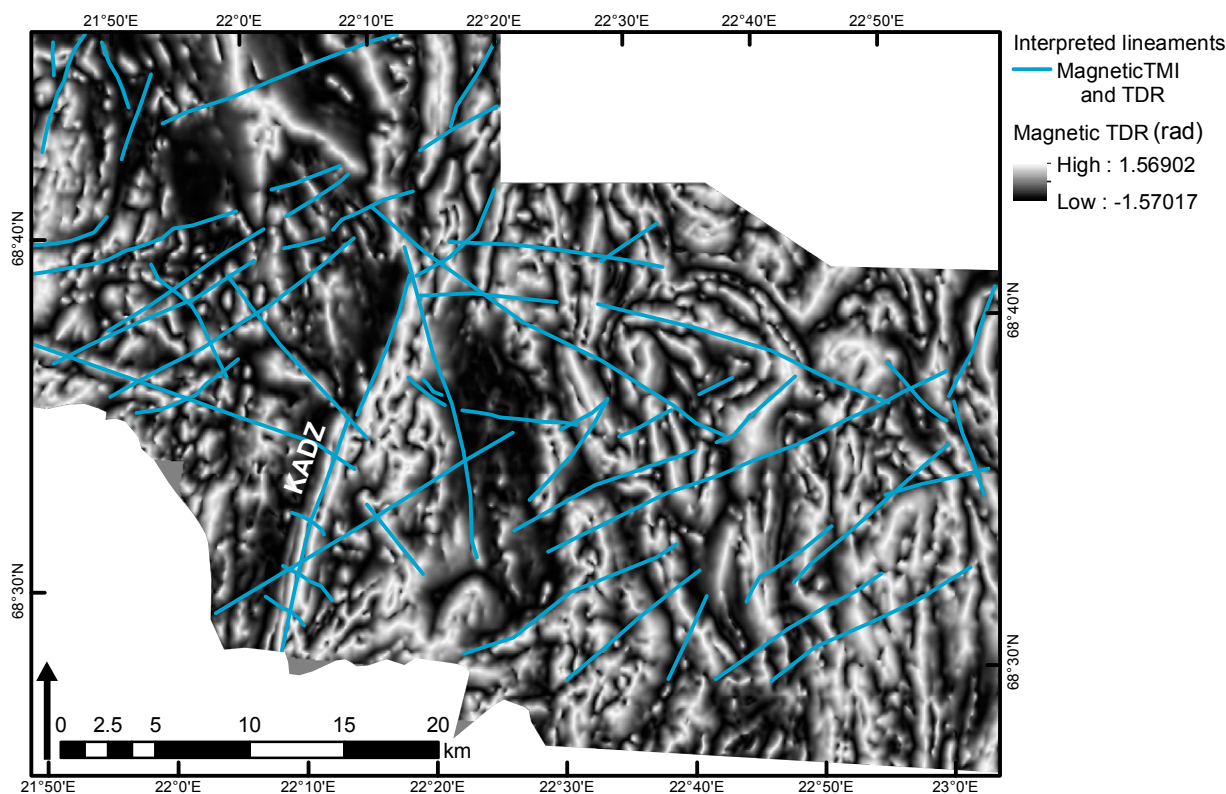


Fig. 7. Visually interpreted structural lines on top of the tilt derivative (TDR) of airborne magnetic data reduced to pole. Alternative location of the Karesuando-Arjeplog deformation zone (KADZ). Geographic coordinates: WGS84. Figure: Maarit Middleton, GTK.

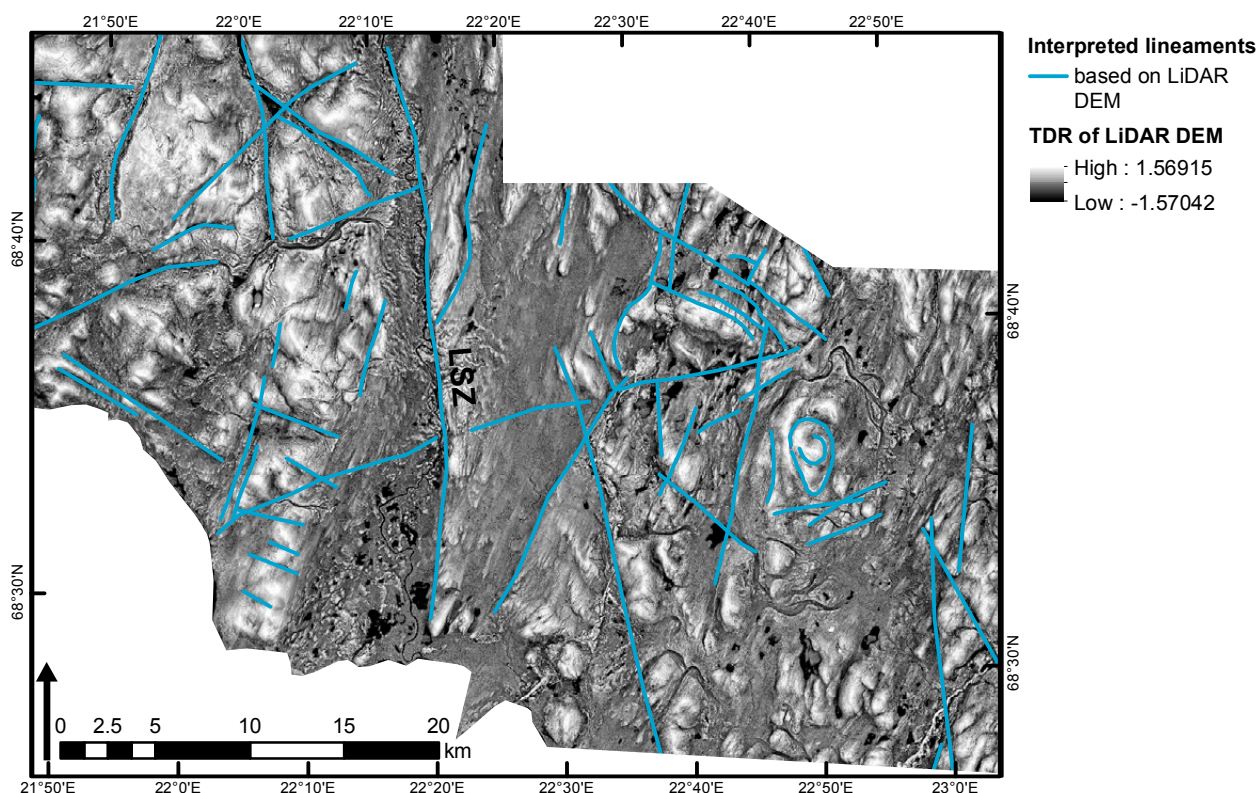


Fig. 8. Visually interpreted structural lines on top of the tilt derivative (TDR) of the digital elevation model (DEM) acquired with airborne laser scanning. The Lätäseno Shear Zone (LSZ described by Karinen et al. 2015) can be only seen as a topographic lineament. Original laser scanned point cloud by @ National Land Survey of Finland, 2013 (license v. 1.0 - 1.5.2012). Geographic coordinate system: WGS84. Figure: Maarit Middleton, GTK.

depressions in the shear zones are a result of the weathering of rocks. In addition, weakness zones are enhanced by glacial activity and post-glacial fluvial activities. The most prominent of the topographic lineaments is the Lätäseno Shear Zone (LSZ) described by Karinen et al. (2014). In addition, approximately 10 km east of the LSZ is another topographic lineament oriented NW–SE, which is less continuous and less prominent in height. The importance of the topographic lineament interpretation is evident in cases like the LSZ, because it cannot be clearly detected from the magnetic data. Because the LSZ has no magnetic response or the response is insignificant, i.e. narrow or low in amplitude, it was not detected with the available airborne magnetic data.

Semi-automatic detection of lineaments from LiDAR DEM was not attempted in this study. Investigations into adopting the image processing

methods, e.g. similar to those suggested by Rutzinger et al. (2007), should be conducted in the future. The TDR of DEM was found to be a valuable tool in visual lineament detection, as it also normalizes the effect of height, thus enhancing the low formations similarly to high ones (see discussion e.g. Smith & Clark 2005). Another advantage of TDR is that it is not biased by an azimuthal component compared to several other visualization filters of DEMs. A number of edge detection filters have been found to enhance the abrupt changes in elevation. However, the challenge is to develop an edge tracing method that would find lineaments, because long continuous elevation features are also created through many other processes. In addition, similarly to the magnetic data, topographic lineaments may be discontinuous in DEM, and the problem of connecting sparsely located linear segments together will therefore be faced.

## CONCLUSIONS

In the long term, the focus in lineament detection should be directed towards increasing the objectivity and being able to produce semi-automated interpretations for the structural geologist who, in turn, could focus on verification and classification of the linear features through field work and drilling rather than lineament digitization. Complete automatization of lineament detection might not be possible, but the focus should be on developing pattern recognition techniques to produce a more objective starting point for geological lineament detection. Currently, linear features in airborne magnetic data with a strong to medium response can be detected with a variety of semi-automated techniques, including object-based methods as demonstrated in this paper. The key role of semi-automated techniques should be in highlighting the existing subtle features that are laborious to detect visually. From this perspective, the CNL lineament detection algorithm OBDL developed in this study for detecting magnetic TDR minima works, although it is not quite as sensitive to the weakest structures as curvature analysis presented by Phillips et al. (2007). In this first attempt to use the OBIA environment for 'worming', it was found that the OBIA algorithm was not quite as sensitive as 'worming' by curvature analysis, because the subtle linear features cannot be emphasized well enough with filtering for segmentation.

The 'worming' approach using curvature analysis (Phillips et al. 2007) or the OBLD algorithm attempts to bring out linear features related to weakness zones, i.e. fracture zones. From the mineral exploration point of view, the least discernible fracture zones in the data might be equally important to the apparent ones. As a general conclusion of this study, data should always be treated with a number of transformations and visualization techniques, such as 'worming', prior to and during edge detection, and edge tracing techniques should be applied for preinterpretation, even though they could not produce complete results. However, currently only visual inspection has been successfully used to reveal linear patterns connecting far apart located short discontinuities in remotely sensed

data. Thus, visual interpretation techniques are still needed to connect breaks in data across raster data containing no physical response or only having a weak response to bedrock fractures. The human eye still exceeds computers in connecting discontinuities over long distances. Therefore, in our understanding, visual lineament detection cannot yet be replaced by pattern recognition.

Because the reliability of lineaments detected from different sources is not well understood, the current focus should be on the interpretation of a variety of data sources. Besides airborne magnetic and DEMs, airborne frequency-domain electromagnetic, regional field gravity data, remotely sensed optical data and airborne gamma-ray surveys should also be included. In Finland, the use of topographic data, especially the LiDAR-produced DEM, will soon be possible anywhere, since by 2019 this high-resolution data source will be available for the entire country.

For future work in mineral exploration, we suggest a holistic approach to regional lineament detection. Lineaments should be interpreted from a variety of remotely sensed data sources, data transformations and edge detection techniques, because each dataset may provide additional information for lineament interpretation. Isaksson et al. (2004) proposed an integrated lineament interpretation approach for geophysical and topographic data sources in radioactive waste repository studies. Each data source was interpreted separately, and in the end, a coordinated interpretation was provided where structural lines describing the same linear feature were linked into a single lineament. A similar approach should be adopted to structural work related to mineral exploration, because every structural hint might be significant and therefore structures giving a weak response might be equally important to those with a strong physical response. Besides mineral exploration, the proposed developments in lineament detection might also benefit groundwater exploration (Sander 2007, Mäkelä 2012), radioactive waste repository studies (e.g. Paananen 2013), infrastructure planning and construction (Airo & Wennerström 2010).

## ACKNOWLEDGEMENTS

Funding for the project was provided from the Tekes Green Mining Programme for the project 'Novel Technologies for Green Field Exploration' (2012–2014). We thank GTK researchers Tero Niiranen for sharing expertise on ore genesis and Jukka Konnunaho and Tuomo Karinen on Enontekiö geology, Mika Larronmaa for producing the LiDAR DEM, Hanna Leväniemi for sharing tips

on the GX and Connect points tools in Oasis, and Ilkka Lahti, Heikki Salmirinne and Juhani Ojala for valuable comments. We also thank Heli Laaksonen at NLS for providing info on the LiDAR data acquisition. Special thanks go to Hanna Leväniemi and Markku Paananen for reviewing the manuscript.

## REFERENCES

- Abarca, M. A. A. 2006.** Lineament extraction from digital terrain models. Case Study San Antonio del Sur Area, South-Easter Cuba. Enschede, the Netherlands: International Institute for Geo-Information Science and Earth Observation. 62 p., 2 appendixes. (dissertation, electronic publication). Available at: [http://www.itc.nl/library/papers\\_2006/msc/ereg/arenas.pdf](http://www.itc.nl/library/papers_2006/msc/ereg/arenas.pdf)
- Abdullah, A., Nassr, S. & Ghaleeb, A. 2013.** Landsat ETM-7 for Lineament Mapping using Automatic Extraction Technique in the SW part of Taiz area, Yemen. *Global Journal of Human Social Science: Geography, Geo-Sciences, Environmental & Disaster Management* 13 (3). (Electronic publication). Available at: <http://socialscienceresearch.org/index.php/GJHSS/article/view/778>.
- Airo, M.-L. & Wennerström, M. 2010.** Application of regional aeromagnetic data in targeting detailed fracture zones. *Journal of Applied Geophysics* 71, 62–70.
- Airo, M.-L. & Leväniemi, H. 2012.** Geophysical structures with gold potential in southern Finland. In: Grönholm, S. & Kärkkäinen, N. (eds) *Gold in Southern Finland: Results of GTK studies 1998-2011*. Geological Survey of Finland, Special Paper 52, 227–244.
- Argialas, D. P. & Mavrantza, O. D. 2004.** Comparison of edge detection and Hough transform techniques for the extraction of geologic features. In: Altan, O. (ed.) *Proceedings XXth ISPRS Congress of the International Society of Photogrammetry and Remote Sensing, 12-23 July 2004, Istanbul, Turkey*. ISPRS Archives XXXV (Part B3), 790–795. (Electronic publication). Available at: <http://www.isprs.org/proceedings/XXXV/congress/comm3/papers/376.pdf>
- Aydogan, D. 2011.** Extraction of lineaments from gravity anomaly maps using the gradients calculation: Application to Central Anatolia. *Earth Planets Space* 63, 903–913.
- Beauchemin, M. & Lamontagne, M. 2011.** A Semi-Automated Method for Lineament Extraction in Aeromagnetic and DEM Data. In: Piwowar, J. M. (ed.) *Proceedings of The Prairie Summit, Regina, Canada, June 1-5 2010*. Regina: Department of Geography, 45–48. (Electronic publication). Available at: [http://uregina.ca/prairies/assets/PrairieSummit\\_Proceedings.pdf](http://uregina.ca/prairies/assets/PrairieSummit_Proceedings.pdf)
- Bedrock of Finland – DigiKP.** Digital map database [Electronic resource]. Espoo: Geological Survey of Finland [referred 6.10.2014]. Version 1.0. Available at: <http://www.geo.fi/en/bedrock.html>
- Bergman, S., Kübler, L. & Martinsson, O. 2001.** Description of regional geological and geophysical maps of northern Norrbotten County (east of the Caledonian orogen). *Sve-riges Geologiska Undersökning, Ba 56*. 110 p.
- Bierlein, F. P., Murphy, F. C., Weinberg, R. F. & Lees, T. 2006.** Distribution of orogenic gold deposits in relation to fault zones and gravity gradients: targeting tools applied to the Eastern Goldfields, Yilgarn Craton, Western Australia. *Mineralium Deposita* 41, 107–126.
- Blaschke, T., Lang, S. & Hay, G. J. (eds) 2008.** *Object-Based Image Analysis. Spatial Concepts for Knowledge-Driven Remote Sensing Applications*. Berlin: Springer-Verlag. 801 p.
- Dillabaugh, C., Niemann, K. & Richardson, D. 2002.** Semi-automated extraction of rivers from digital imagery. *Geoinformatica* 6 (3), 263–284.
- Debeglia, N., Martelet, G., Perrin, J., Truffert, C., Ledru, P. & Tourlière, B. 2006.** Semi-automated structural analysis of high resolution magnetic and gamma-ray spectrometry airborne surveys. *Journal of Applied Geophysics* 58, 13–28.
- eCognition Community.** [www-pages] Munich: Trimble Geospatial [accessed 14.1.2014]. Available at: [community.ecognition.com](http://community.ecognition.com)
- Fairhead, J. D. & Williams, S. E. 2006.** Evaluating normalized magnetic derivatives for structural mapping. *SEG Technical Program Expanded Abstracts* 01/2006, 25(1), 845–849. (Electronic publication). Available at: <http://library.seg.org/doi/abs/10.1190/1.2370388>
- Fitton, N. C. & Cox, S. J. D. 1998.** Optimising the application of the Hough transform for automatic feature extraction from geoscientific images. *Computers & Geosciences* 24 (10), 933–951.
- Gloauguen, R., Marpu, P. R. & Niemeier, I. 2007.** Automatic extraction of faults and fractal analysis from remote sensing data. *Nonlinear Processes in Geophysics* 14, 131–138.
- Grant, F. S., 1984.** Aeromagnetics, geology and ore environments, I: Magnetite in igneous, sedimentary and metamorphic rocks: an overview. *Geoexploration* 23, 303–333.
- Gruen, A. & Li, H. 1997.** Semi-automatic linear feature extraction by dynamic programming and LSB-snakes. *Photogrammetric Engineering & Remote Sensing* 63 (8), 985–995.
- Hautaniemi, H., Kurimo, M., Multala, J., Leväniemi, H. & Vironmäki, J. 2005.** The "Three In One" aerogeophysical concept of GTK in 2004. In: Airo, M.-L. (ed.) *Aerogeophysics in Finland 1972–2004: Methods, System Characteristics and Applications*. Geological Survey of Finland, Special Paper 39, 21–74.
- Henkel, H. & Guzmán, M. 1977.** Magnetic features in fracture zones. *Geoexploration* 15, 173–181.

- Hobbs, W. H. 1904.** Lineaments of the Atlantic border region. *Geological Society of America Bulletin* 15, 483–506.
- Hooper, D. M., Bursik, M. I. & Webb, F. H. 2003.** Application of high-resolution, interferometric DEMs to geomorphic studies of fault scarps, Fish Lake Valley, Nevada–California, USA. *Remote Sensing of Environment* 84 (2), 255–267.
- Hornby, P., Boschetti, F. & Horowitz, F. G. 1999.** Analysis of potential fields data in the wavelet domain. *Geophysical Journal International* 137, 175–196.
- Isaksson, H., Thunehed, H. & Keisu, M. 2004.** Forsmark site investigation. Interpretation of airborne geophysics and integration with topography. *Svensk Kärnbränslehantering AB, SKB P-04-29*. 71 p. (Electronic publication). Available at: [http://www.posiva.fi/files/1061/WR2005-34\\_web.pdf](http://www.posiva.fi/files/1061/WR2005-34_web.pdf)
- Karinen, T., Lahti, I. & Konnunaho, J. 2015.** 3D/4D geological modelling of the Hietakero and Vähäkirkkio areas in the Lätäseno Schist Belt, Enontekiö, northern Finland. In: Sarala, P. (ed.) *Novel technologies for greenfield exploration*. Geological Survey of Finland, Special Paper 57, 121–134. (this journal)
- Kirbas, C. & Queck, F. 2003.** A review of vessel extraction techniques and algorithms. *AMC Computing Surveys (CSUR)*, 36 (2), 81–121.
- Kocal, A., Duzgun, H. S. & Karpuz, C. 2007.** An accuracy method for the remotely sensed discontinuities: a case study in Andesite Quarry area, Turkey. *International Journal of Remote Sensing* 28 (17), 3915–3936.
- Koike, K., Nagano, S. & Ohm, M. 1995.** Lineament analysis of satellite images using a segment tracing algorithm (STA). *Computers & Geosciences* 21 (9), 1091–1104.
- Koike, K., Nagano, S. & Kawaba, K. 1998.** Construction and analysis of interpreted fracture planes through combination of satellite-image derived lineaments and digital elevation model data. *Computers & Geosciences* 24 (6), 573–583.
- Korhonen J. 2005.** Airborne Magnetic Method: Special Features and Review on Applications. In: Airo, M.-L. (ed.) *Aerogeophysics in Finland 1972–2004. Methods, System Characteristics and Applications*. Geological Survey of Finland, Special Paper 39, 77–102.
- Lahti, I. & Karinen, T. 2010.** Tilt derivative multiscale edges of magnetic data. *The Leading Edge* 29 (1), 24–29.
- Lahti, I., Nykänen, V. & Niiranen, T. 2014.** Gravity worms in the exploration of epigenetic gold deposits: New insight into the prospectivity of the central Lapland Greenstone Belt, northern Finland. In: Niiranen, T., Lahti, I., Nykänen, V. & Karinen, T. (eds) *Central Lapland Greenstone Belt 3D modeling project. Final Report*. Geological Survey of Finland, Report of Investigation 209, 8–17.
- Leväniemi, H. 2011.** Geofysikaalisten rasteriaineistojen rakkennetulkintatyökaluja Geosoft Oasis Montaj -ohjelmistolle. Geological Survey of Finland, Report 48/2011. 27 p. (Electronic publication). Available at: [http://tupa.gtk.fi/raportti/arkisto/48\\_2011.pdf](http://tupa.gtk.fi/raportti/arkisto/48_2011.pdf) (in Finnish)
- Mäkelä, J. 2012.** Drilled well yield and hydraulic properties in the Precambrian crystalline bedrock of Central Finland. *Turku: Annales Universitatis Turkuensis AII* (267). 353 p, 3 appendixes. (dissertation, Electronic publication). Available at: <http://urn.fi/URN:ISBN:978-951-29-4973-1>
- Marpu, P. R., Niemeyer, I., Nussbaum, S. & Gloaguen, R. 2008.** A procedure for automatic object-based classification. In: Blaschke, T., Lang, S. & Hay, G. J. (eds) *Object-Based Image Analysis. Spatial Concepts for Knowledge-Driven Remote Sensing Applications*. Berlin: Springer-Verlag, 169–184.
- Mavranza, O. & Argialas, D. 2008.** An object-oriented image analysis approach for the identification of geologic lineaments in a sedimentary geotectonic environment. In: Blaschke, T., Lang, S. & Hay, G. J. (eds) *Object-Based Image Analysis. Spatial Concepts for Knowledge-Driven Remote Sensing Applications*. Berlin: Springer-Verlag, 383–398.
- Mertanen, S., Airo, M.-L., Elminen, T., Niemelä, R., Pajunen, M., Wasenius, P. & Wennerström, M. 2008.** Paleomagnetic evidence for Mesoproterozoic-paleozoic reactivation of the paleoproterozoic crust in Southern Finland. In: Pajunen, M. (ed.) *Tectonic evolution of the Svecofenian crust in southern Finland – a basis for characterizing bedrock technical properties*. Geological Survey of Finland, Special Paper 47, 215–252.
- Miller, H. G. & Singh, V. 1994.** Potential field tilt - A new concept for location of potential field sources. *Journal of Applied Geophysics* 32, 213–217.
- Ojala, V. J., Kuivamäki, A. & Vuorela, P. 2004.** Postglacial deformation of bedrock in Finland. Geological Survey of Finland, Nuclear Waste Disposal Research, Report YST-120. 23 p. (Electronic publication). Available at: [http://tupa.gtk.fi/julkaisu/ydinjate/yst\\_120.pdf](http://tupa.gtk.fi/julkaisu/ydinjate/yst_120.pdf)
- O’Leary, D. W., Freidman, J. D. & Pohn, H. A. 1976.** Lineament, linear, lineation: Some proposed new definitions for old terms. *Geological Society of America Bulletin* 87, 1463–1469.
- Olesen, O., Dehls, J.F., Ebbing, J., Henriksen, H., Kihle, O. & Lundin, E. 2006.** Aeromagnetic mapping of deep-weathered fracture zones in Oslo Region - a new tool for improved planning of tunnels. *Norwegian Journal of Geology* 87, 253–267.
- Ouzounov, D., Bryant, N., Logan, T., Pulinets, S. & Taylor, P. 2006.** Satellite thermal IR phenomena associated with some of the major earthquakes in 1999–2003. *Physics and Chemistry of the Earth* 31, 154–163.
- Paananen, M. 2013.** Completed Lineament Interpretation of the Olkiluoto Region. Posiva, Posiva Report 2013-02. 99 p., 2 attachments. (Electronic publication). Available at: [http://www.posiva.fi/files/3402/POSIVA\\_2013-02.pdf](http://www.posiva.fi/files/3402/POSIVA_2013-02.pdf)
- Pagel, M. & Leroy, J. L. (eds) 1991.** Source, Transport and Deposition of Metals. Chapter 5. Structural environment. Rotterdam, Netherlands: A.A. Balkema, 419–500.
- Papadaki, E. S., Mertikas, S. P. & Sarris, A. 2011.** Identification of lineaments with possible structural origin using ASTER images and DEM derived products in Western Crete, Greece. *EARSeL Proceedings* 10 (1/2011), 9–26. (Electronic publication). Available at: [http://www.e-proceedings.org/static/vol10\\_1/10\\_1\\_papadaki1.pdf](http://www.e-proceedings.org/static/vol10_1/10_1_papadaki1.pdf)
- Phillips, J. D. 2007.** Geosoft eXecutables (GX’s) developed by the U.S. Geological Survey, version 2.0, with notes on GX development from Fortran code. U.S. Department of the Interior, U.S. Geological Survey, Open-File Report 2007-1355. 111 p. (Electronic Resource) Available at : <http://pubs.usgs.gov/of/2007/1355/pdf/of07-1355.pdf>
- Phillips, J. D., Hansen, R. O. & Blakely, R. J. 2007.** The use of curvature in potential-field interpretation. *Exploration Geophysics* 38, 111–119.
- Pilkington, M. & Keating, P. B. 2009.** The utility of potential field enhancements for remote predictive mapping. *Canadian Journal of Remote Sensing* 35 (S1), S1–S11.
- Quackenbush, L. J. 2004.** A Review of Techniques for Extracting Linear Features from Imagery. *Photogrammetric Engineering & Remote Sensing* 70 (12), 1383–1392.

- Rahnama, M. & Gloaguen, R. 2014.** TecLines: a MATLAB-Based Toolbox for Tectonic Lineament Analysis from Satellite Images and DEMs, Part 1: Line Segment Detection and Extraction. *Remote Sensing* 6, 5938–5958. (Electronic publication). Available at: <http://www.mdpi.com/2072-4292/6/7/5938>
- Rutzinger, M., Maukisch, M., Petrini-Monteferrri, F. & Stötter, J. 2007.** Development of Algorithms for the Extraction of Linear Patterns (Lineaments) from Airborne Laser Scanning Data. In: Keller-Pirklbauer, A., Keiler, M., Embleton-Hamann, C., Stötter, J. (eds) *Proceedings Geomorphology for the Future, Obergurgl, Austria, 2-7 September 2007*. Innsbruck: Innsbruck University Press, 161–168.
- Sander, P. 2007.** Lineaments in groundwater exploration: a review of application and limitations. *Hydrogeology Journal* 15, 71–74.
- Sander, P., Minor, T. B. & Chesley, M. M. 1997.** Groundwater exploration based on lineament analysis and reproducibility test. *Ground Water* 35 (5), 888–894.
- Smith, M. J. & Clark, C. D. 2005.** Methods for the visualization of digital elevation models for landform mapping. *Earth Surface Processes and Landforms* 30, 885–900.
- Sukumar, M., Vankatesan, N. & Nelson Kennedy Babu, C. 2014.** A Review of Various Lineament Detection Techniques for high resolution Satellite Images. *International Journal of Advanced Research in Computer Science and Software Engineering* 4 (3), 72–78.
- Sutinen, R., Hyvönen, E. & Kukkonen, I. 2014.** LiDAR detection of paleo-landslides in the vicinity of the Suasselkä postglacial fault, Finnish Lapland. *International Journal of Applied Earth Observation and Geoinformation* 27 (Part A), 91–99.
- Torppa, J., Middleton, M., Hyvönen, E., Lerssi, J. & Fraser, S. 2015.** A novel spatial analysis approach for assessing regional-scale mineral prospectivity in northern Finland. In: Sarala, P. (ed.) *Novel technologies for greenfield exploration*. Geological Survey of Finland, Special Paper 57, 87–120. (this journal)
- Verduzco, B., Fairhead, J. D. & Green, C. M. 2004.** New insights into magnetic derivatives for structural mapping. *The Leading Edge* 23 (2), 116–119.